Synthesis and Reactivity Studies of a [Cp*Rh] Complex Supported by a Methylene-Bridged Hybrid Phosphine-Imine Ligand

Julie A. Hopkins,[#] Davide Lionetti,[#,†] Victor W. Day,[#] and James D. Blakemore[#,*]

Department of Chemistry, University of Kansas, 1567 Irving Hill Road, Lawrence, KS 66045, United States

Supporting Information Placeholder

Abstract

[Cp*Rh] complexes (Cp* = η^5-pentamethylcyclopentadienyl) supported by bidentate chelating ligands are useful in studies of redox chemistry and catalysis, but little information is available for derivatives bearing "hybrid" [*P,N*] chelates. Here, the preparation, structural characterization, and chemical and electrochemical properties of a [Cp*Rh] complex bearing the κ^2-[*P*,*N*]-2-[(diphenylphosphino)methyl]pyridine ligand (PN) are reported. Cyclic voltammetry data reveal that [Cp*Rh(PN)Cl]PF_6 (**1**) undergoes a chemically reversible, net two-electron reduction at –1.28 V vs. ferrocenium/ferrocene, resulting in generation of a rhodium(I) complex (**3**) that is stable on the timescale of the voltammetry. However, ^{1}H and ^{31}P{^{1}H} NMR studies reveal that chemical reduction of **1** generates a mixture of products over a 1 h timescale; this mixture forms as a result of deprotonation of the methylene group of **1** by **3** followed by further reactivity. The analogous complex [Cp*Rh(PQN)Cl]PF_6 (**2**; PQN = κ^2-[*P*,*N*]-8-(diphenylphosphino)quinoline) does not undergo self-deprotonation or further reactivity upon two-electron reduction, confirming the reactivity of the acidic backbone methylene C–H bonds in the PN complexes. Comparison of the electrochemical properties **1** and **2** also shows that the extended conjugated system of PQN contributes to an additional ligand-centered redox event for **2** that is absent for **1**.

1. Introduction

Identification of ligand structure-function relationships is an important strategy for rational design of organometallic catalysts. In redox chemistry, substitution of one ligand for another often results in significant changes to the properties of the target metal complex, for example in shifted reduction potential, reactivity, or basicity.[1] Such shifts can often lead to marked changes in catalytic effectiveness, especially in molecular catalysis of small-molecule activation reactions requiring effective management of both protons (H^+) and reducing equivalents (e^-). Efforts to understand how ligands impact transfer of H^+/e^- form the basis of strategies aimed at tuning of catalysts and improving catalytic efficiencies.[2] However, these efforts remain challenging due to the propensity of both metal centers and ligands to become directly involved in reactivity.[3]

We have been working to understand the reactivity properties of a model family of organometallic rhodium complexes that can serve, in several cases, to couple H^+/e^- equivalents and catalyze production of H_2. The complexes are supported by the η^5-pentamethylcyclopentadienyl (Cp*) ligand, as well as an additional bidentate ligand. The parent catalyst in this family, [Cp*Rh(bpy)Cl]$^+$ (**A**, Chart 1), is supported by the workhorse 2,2′-bipyridyl (bpy) ligand. This complex was reported in 1987 by Kölle and Grätzel as a catalyst for H_2 production,[4] and by other groups to serve as a catalyst for NAD^+ reduction to NADH.[5] For many years, this catalyst was presumed to operate via a rhodium(III) hydride intermediate, although such a species had not been isolated or fully characterized. New interest in this species was piqued by reports from our group[6] and others[7] showing that exposure of the reduced form of **A**, Cp*Rh(bpy), to weak proton sources results in generation of an isolable compound bearing the *endo*-η^4-pentamethylcyclopentadiene ligand (η^4-Cp*H), generated by transfer of H^+ to the Cp* ring.[8,9] (*n.b.*, the *endo* face of the ring is defined as the one facing the metal center). Related reactivity studies have demonstrated that the exposure of the compound bearing (η^4-Cp*H) to a sufficiently strong acid results in quantitative generation of H_2 and regeneration of (η^5-Cp*). Inspired by this rather uncommon chemistry, we have been investigating synthesis and reactivity of other [Cp*Rh] complexes supported by various bidentate ligands

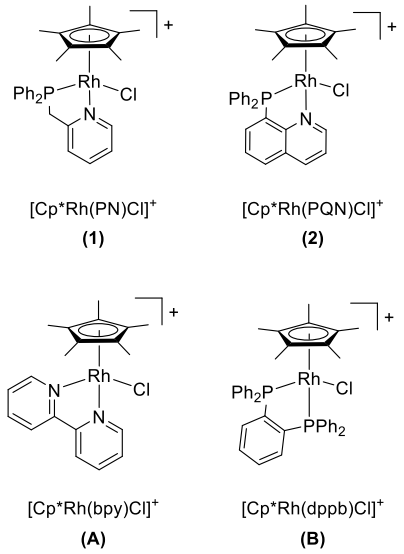

Chart 1. Series of half-sandwich rhodium complexes.

Along this line, we have shown that reduction and protonation of a [Cp*Rh] complex (**B**) bearing the 1,2-bis(diphenylphosphino)benzene (dppb) ligand affords access to a stable rhodium(III) hydride.[10] Unlike the [η^4-Cp*H] complexes mentioned above, this [Rh^{III}–H] complex is remarkably resistant to protonolysis.[6,7,11,12] This result agrees with the high apparent stability of other half-sandwich rhodium hydride complexes studied in different contexts,[13] as well as the reactivity properties of rhodium hydrides supported by other ligand sets.[14] However, the high stability of the dppb-supported hydride renders it somewhat less applicable to model studies of more reactive [Cp*Rh] systems.

More recently, we have reported the synthesis and reactivity of a [Cp*Rh] complex (**2**) supported by a hybrid ligand, 8-(diphenylphosphino)quinoline (PQN).[15] PQN presents a triarylphosphine donor and an imine donor with appropriate placement for binding to [Cp*Rh] in a five-membered metallacycle. Use of PQN engenders intriguing properties that are intermediary between those of systems bearing diimine ligands and dppb. In particular, use of PQN favors generation of an isolable [Rh^{III}–H] species that can, unlike its dppb analogue, undergo protonolysis and evolve H_2 (see Scheme 1). Moreover, **2** displays especially rich reductive electrochemistry, undergoing a two-electron reduction to form Cp*Rh(PQN) at –1.19 V vs. $Fc^{+/0}$ (all potentials referenced to ferrocenium/ferrocene, denoted hereafter as $Fc^{+/0}$) that can be further reduced by one electron at –2.26 V vs. $Fc^{+/0}$.

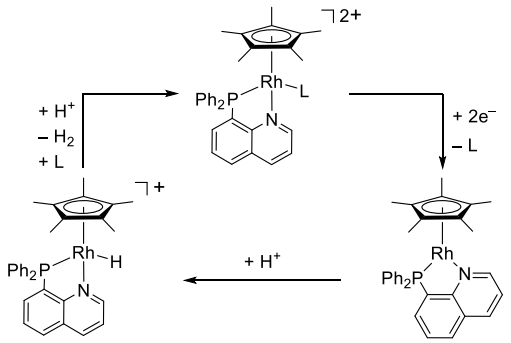

Scheme 1. H_2 evolution chemistry with the Cp*Rh(PQN) platform.

Despite these features, the only [Cp*Rh] system supported by a hybrid [*P*,*N*] chelating ligand that has been investigated for its reactivity properties is this example bearing PQN.[15] Because of the especially useful properties engendered by this donor set, we imagined that probing the synthesis and reactivity profile of [Cp*Rh] species supported by other hybrid [*P*,*N*] ligands could be a useful strategy for understanding the reactivity properties of this family of compounds. Along this line, our attention was drawn to the κ^2-[*P*,*N*]-2-[(diphenylphosphino)methyl]pyridine ligand, commonly known as PN; this ligand is chelating, much like PQN, but presents an alkyldiarylphosphine donor and an imine donor for binding to a central metal. Importantly, although the coordination chemistry of PN ligands has been studied with a variety of transition metals,[16] only a few Rh complexes supported by PN are known.[17] In particular, we were pleased to find that structural data from X-ray diffraction (XRD) analysis was available in the Cambridge Structural Database[18] for [Cp*Rh(PN)Cl]PF_6 (**1**),[19] suggesting that this compound could be prepared. However, no information on the synthetic methods needed for preparation of **1** or information regarding its properties are available, encouraging further work to establish how its reactivity compares with other members of our family of complexes from previous studies.

Here, we report the synthetic procedures, characterization data, and reactivity studies of the

[Cp*Rh] complex **1** supported by PN. New structural data for **1** from XRD are compared both to that previously available[19] as well as to our prior data for the PQN-ligated analogue **2**;[15] these analyses suggest that PN is a slightly more effective donor than PQN to Rh. Consistent with this structural data, **1** undergoes a net two-electron reduction near –1.28 V vs. $Fc^{+/0}$, a value that is significantly more negative than that of **2**, resulting in generation of a transient rhodium(I) complex (**3**) that is stable on the timescale of voltammetry. **3** displays no further reductions in our accessible solvent window. Chemical reduction of **1** with Na(Hg), however, does not yield **3** as an isolable compound; rather, a mixture of products forms as a result of further reactivity leading to generation of several observable compounds that has been studied by ^{1}H and $^{31}P\{^{1}H\}$ nuclear magnetic resonance (NMR). Taken together, the results suggest that the highly basic nature of **3** and the acidic backbone C–H bonds of PN engender unexpected reactivity upon chemical reduction of **1** that is unavailable in **2**, which lacks acidic backbone protons. Avoidance of acidic moieties in supporting ligands is thus a strategy that can guide future work with highly basic [Cp*Rh] complexes intended for study of H^{+}/e^{-} management in catalysis.

2. Experimental

2.1 General Considerations

All manipulations were carried out in dry N_2-filled gloveboxes (Vacuum Atmospheres Co., Hawthorne, CA) or under N_2 atmosphere using standard Schlenk techniques unless otherwise noted. All solvents were of commercial grade and dried over activated alumina using a PPT Glass Contour (Nashua, NH) solvent purification system prior to use, and were stored over molecular sieves. All chemicals were from major commercial suppliers and used as received after extensive drying. $[Cp^*RhCl_2]_2$ was prepared according to literature procedure.[20] The PN ligand was synthesized by the method of Hung-Low.[21] Deuterated NMR solvents were purchased from Cambridge Isotope Laboratories; CD_3CN was dried over molecular sieves and C_6D_6 was dried over sodium/benzophenone. ^{1}H, ^{13}C, and ^{31}P NMR spectra were collected on 400 or 500 MHz Bruker spectrometers and referenced to the residual protio-solvent signal[22] in the case of ^{1}H and ^{13}C. Heteronuclear NMR spectra were referenced to the appropriate external standard following the recommended scale based on ratios of absolute frequencies (Ξ).[23]

2.2 Electrochemistry

Electrochemical experiments were carried out in a nitrogen-filled glove box. 0.10 M tetra(n-butylammonium)hexafluorophosphate (Sigma-Aldrich; electrochemical grade) in acetonitrile served as the supporting electrolyte. Measurements were made with a Gamry Reference 600 Plus Potentiostat/Galvanostat using a standard three-electrode configuration. The working electrode was the basal plane of highly oriented pyrolytic graphite (HOPG) (GraphiteStore.com, Buffalo Grove, Ill.; surface area: 0.09 cm^2), the counter electrode was a platinum wire (Kurt J. Lesker, Jefferson Hills, PA; 99.99%, 0.5 mm diameter), and a silver wire immersed in electrolyte served as a pseudo-reference electrode (CH Instruments). The reference was separated from the working solution by a Vycor frit (Bioanalytical Systems, Inc.). Ferrocene (Sigma Aldrich; twice-sublimed) was added to the electrolyte solution at the conclusion of each experiment (~1 mM); the midpoint potential of the ferrocenium/ferrocene couple (denoted as $Fc^{+/0}$) served as an external standard for comparison of the recorded potentials. Concentrations of analyte for cyclic voltammetry were typically 1 mM.

2.3 Crystallography

A full hemisphere of diffracted intensities (560 5-second frames with an ω scan width of 1.00°) was measured for a single-domain crystal of **1** using graphite-monochromated Mo Kα radiation (λ = 0.71073 Å) on a Bruker SMART APEX CCD Single Crystal Diffraction System. X-rays were provided by a fine-focus sealed X-ray tube operated at 50 kV and 35 mA. Preliminary lattice constants were determined with the Bruker program SMART.[24] The Bruker program SAINT[25] was used to produce integrated reflection intensities from the frames and determine final lattice constants using 8486 peak centers. The data set was corrected empirically for variable absorption effects using equivalent reflections. The Bruker software package SHELXTL was used to solve the structure using "direct methods" techniques. All stages of weighted full-matrix least-squares refinement were conducted using Fo_2 data with the v2014.11-0 software package.[26] Relevant crystallographic and

refinement data are given in Table S1 of the Supporting Information document.

The final structural model for **1** incorporated anisotropic thermal parameters for all nonhydrogen atoms and isotropic thermal parameters for all hydrogen atoms. All non-methyl hydrogen atoms were fixed at idealized riding model sp^2- or sp^3-hybridized positions with C-H bond lengths of 0.94 or 0.97 Å. All five [Cp*] methyl groups were incorporated into the structural model as sp^3-hybridized rigid groups with C-H bond lengths of 0.98 Å that were allowed to rotate freely about their C-C bonds in least-squares refinement cycles. The isotropic thermal parameters of all hydrogen atoms were fixed at values 1.2 (nonmethyl) or 1.5 (methyl) times the equivalent isotropic thermal parameter of the carbon atom to which they are covalently bonded.

2.4 Synthesis

2.4.1 Synthesis of 2-[(Diphenylphosphino)methyl]pyridine

PN was synthesized according to a modified literature procedure.[21] A solution of n-butyllithium in tetrahydrofuran (2.03 mL, 2.65 mmol, 1 equiv.) was added to a "thawing" sample of 2-picoline in tetrahydrofuran (0.500 g, 5.4 mmol, 1 equiv.) that had been previously frozen at in a cold well in an inert atmosphere glovebox with liquid nitrogen (–196 °C). Allowing the sample to melt upon addition of the n-butyllithium solution over 20 min resulted in a bright orange solution. This solution containing n-butyllithium and 2-picoline was then refrozen in the same manner, and subsequently a solution of chlorodiphenylphosphine in tetrahydrofuran (1.185 g, 5.37 mmol, 1 equiv.) was added. Allowing the mixture to warm to room temperature and stir for 2 h yielded a bright yellow solution. The solution was filtered, and volatiles removed *in vacuo* to yield a dark orange solid. Direct extraction with hexane (without use of an acid/base extraction step as previously called for in ref. 21) and removal of the volatiles *in vacuo* yielded a useful quantity of an air-sensitive white solid. (Yield: 0.385 g, 26%) Spectroscopic data for the isolated material agreed with those previously reported for PN.[27]

*2.4.2 Synthesis of **1***

To a suspension of $[Cp^*RhCl_2]_2$ in acetonitrile (0.110 g, 0.177 mmol, 1.0 equiv.) were added $AgPF_6$ (0.180 g, 0.712 mol, 2 equiv.) and PN (0.097 g, 0.0348 mmol, 2.05 equiv.) as acetonitrile solutions. The color of the reaction mixture rapidly changed from brick-red to orange, and a yellow precipitate formed. After 15 min, the suspension was filtered to remove the AgCl byproduct, and the volume of the filtrate was reduced to ca. 1 mL. Addition of diethyl ether (ca. 20 mL) caused precipitation of a yellow solid, which was collected by filtration (0.0456 g, 38%). Vapor diffusion of diethyl ether into a concentrated acetonitrile solution of the product yielded single-crystals of **1** suitable for X-ray diffraction studies. ^{1}H NMR (500 MHz, CD_3CN) δ 8.61 (d, J = 5.7 Hz, 1H), 8.01 (t, J = 7.81 Hz, 1H), 7.78 (ddd, J = 11.8, 8.3, 1.4 Hz, 2H), 7.72 – 7.67 (m, 1H), 7.67 – 7.64 (m, 3H), 7.64 – 7.59 (m, 2H), 7.58 – 7.52 (m, 2H), 7.45 (ddd, J = 8.6, 5.3, 2.2 Hz, 2H), 4.43 (dd, J = 17.4, 14.5 Hz, 1H), 4.14 (dd, J = 17.4, 10.7 Hz, 1H), 1.50 (d, J = 3.8 Hz, 15H) ppm. ^{13}C{^{1}H} NMR (126 MHz, CD_3CN) δ 154.84 (s), 141.01 (s), 135.87 (d, J = 10.8 Hz), 133.68 (d, J = 2.84 Hz), 132.85 (d, J = 3.0 Hz), 130.19 (t, J = 9.8 Hz), 126.62 (s), 125.52 (d, J = 10.9 Hz), 102.47 (d, J = 3.0 Hz), 102.42 (d, J = 2.84 Hz), 43.31 (d, J = 34.5 Hz), 9.37 (s), ppm. ^{31}P{^{1}H} NMR (162 MHz, C_6D_6) δ 51.57 (d, J = 140.3 Hz), –144.65 (sep, J = 706.2 Hz) ppm. **1** was found to be acutely air-sensitive and satisfactory elemental analysis could not be obtained. In lieu of elemental analysis, ^{1}H NMR was used to confirm diamagnetic spectroscopic purity.

2.4.3 Chemical Reduction of 1

A suspension of **1** in tetrahydrofuran (0.5 g, 0.717 mmol) was stirred over freshly prepared sodium-mercury amalgam (1% Na in Hg; 0.049 g Na^0, 1.78 mmol, 10 equiv.) and stirred for 48 h, during which time the yellow suspension became a dark blue solution. The mixture was filtered, and the volatiles removed *in vacuo*. Further extraction with hexanes and removal of solvent *in vacuo* yielded a dark blue solid suitable for NMR studies in C_6D_6.

3. Results and Discussion

*3.1 Synthesis and characterization of **1***

The dimeric complex, $[Cp^*RhCl_2]_2$,[20] is useful for straightforward synthesis of [Cp*Rh] complexes with chelating bidentate ligands.[28] For complex **1** addition of 2 equivalents of $AgPF_6$ to 1 equivalent of $[Cp^*RhCl_2]_2$, followed by 2.05 equivalents of free PN ligand results clean generation of complex **1** (Scheme 2).

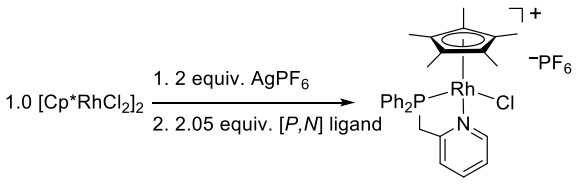

Scheme 2. Synthesis of **1**

The characterization of **1** by proton nuclear magnetic resonance (^{1}H NMR) reveals a signal at 1.50 ppm (integrating to 15H) corresponding to the equivalent protons on [Cp*]; this resonance displays coupling to the phosphorous nucleus ($^4J_{H,P}$ ≈ 3.9 Hz) of the PN ligand. This coupling is assigned as H,P coupling due to the uniform absence of H,Rh coupling for the methyl groups in analogous [Cp*Rh] complexes bearing non-phosphorus-containing bidentate ligands.[11,12,15] Additionally, the ^{1}H NMR of **1** reveals two multiplets at 4.43 and 4.14 ppm (Figure 1, middle spectrum), each integrating to 1H and corresponding to the chemically inequivalent methylene protons on the bidentate [*P,N*] ligand. These multiplets exhibit geminal coupling to each other ($^2J_{H,H}$ ≈ 17.4 Hz) as well as coupling to the phosphorus nucleus ($^2J_{H,P}$ ≈ 14.5 Hz and $^2J_{H,P}$ ≈ 10.7 Hz, respectively) resulting in two doublets of doublets that display the expected "roofing" behavior. For comparison, the ^{1}H{^{31}P} NMR spectrum displays only two doublets at 4.43 and 4.14 ppm ($J_{H,H}$ ≈ 17.4 Hz; see Figure 1, top spectrum). This result confirms the geminal coupling between the chemically inequivalent protons, through decoupling of phosphorus. The "roofing" appearance of the methylene peaks is expected considering that the difference in chemical shift between the chemically inequivalent protons is comparable in magnitude to their chemical coupling ($J_{H,H}$). The ^{1}H NMR spectrum of **2** does not display resonances near 4.25 ppm because the quinoline bridge of the PQN ligand lacks methylene protons.[15]

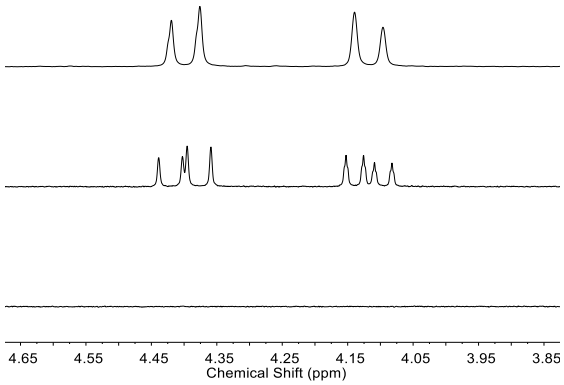

Figure 1. Characterization of **1** and **2**. Upper spectrum: ^{1}H{^{31}P} NMR of **1**; Middle spectrum: ^{1}H NMR of **1** (middle); Lower spectrum: ^{1}H NMR of **2**.

Further characterization of **1** with ^{31}P{^{1}H} NMR (Figure 2, upper spectrum) reveals a doublet at 51.57 ppm ($^1J_{P,Rh}$ ≈ 140.3 Hz), confirming direct bonding between rhodium and the phosphorus atom of PN. For comparison, the ^{31}P{^{1}H} NMR of **2** (Figure 2, lower spectrum) shows a doublet at 47.90 ppm ($^1J_{P,Rh}$ ≈ 143.8 Hz).[15] The more downfield position of the ^{31}P resonances in **1** is indicative of a more electron rich phosphorus atom, suggesting that PN behaves as a more strongly donating ligand in **1** than PQN in **2**.

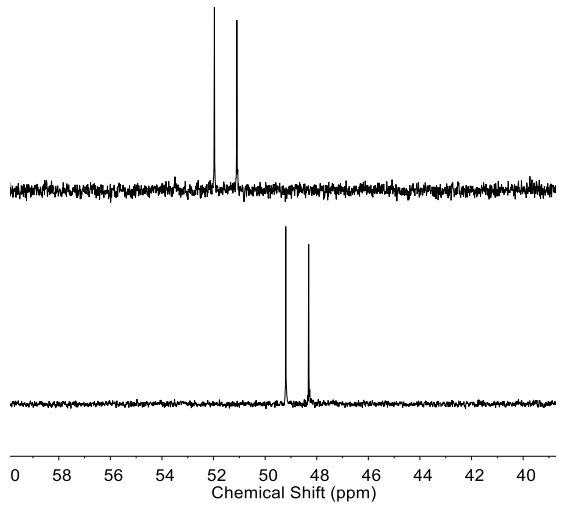

Figure 2. ^{31}P{^{1}H} NMR spectra: **1** (upper) and **2** (lower).

3.2 X-ray Diffraction Studies

As mentioned earlier, we were pleased to find that **1** was previously characterized by XRD analysis and reported to the Cambridge Structural Database as a Private Communication.[19] However,

no description of the origin of the structure or the properties of **1** have been made available in prior work. Thus, we pursued further structural data to provide needed context for the work here, and to obtain information for comparison to the previously reported data.[19] Vapor diffusion of diethyl ether into acetonitrile yielded orange crystals of **1** suitable for X-ray diffraction studies. The resulting solid-state structure reveals the geometry of the formally Rh(III) metal center in **1** to be *pseudo*-octahedral (Figure 3). The first coordination sphere around the metal contains the κ^2-[*P*,*N*] scaffold, a single bound chloride anion, and the [η^5-Cp*] ligand. Notably, there is good agreement between the previously reported structural data and the data from our study; the bond lengths (and their estimated standard deviations, see Table 1) do not differ significantly between the two data sets, confirming that these data are collectively suitable for interpretation here.

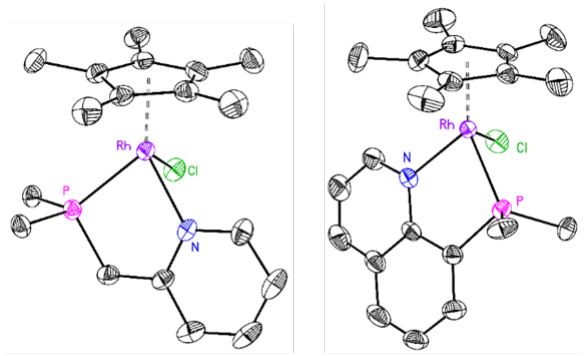

1 **2**

Figure 3. Comparison of the solid-state structures of **1** and **2**.[15] Outersphere hexafluorophosphate (**1**) and triflate (**2**) cournteranions and all hydrogen atoms are omitted for clarity. Phenyl groups are truncated for clarity. Thermal ellipsoids are shown at the 50% probability level.

	1 (new)	**1** (prior work)	**2**
CCDC entry	1973828	233218	1858635
Rh–Cl (Å)	2.416(2)	2.4176(6)	2.402(6)
Rh–P (Å)	2.2730(18)	2.2949(5)	2.3037(6)
Rh–N (Å)	2.119(3)	2.1275(15)	2.122(2)
Rh–Cp_{cent} (Å)	1.832	1.837	1.830
∠P–Rh–N (º)	81.14°	81.36°	82.20°
Reference	this work	Ref. 19	Ref. 15

Table 1. Comparison of bond lengths and angles for complexes **1** and **2**.

From inspection of our new structural data, the angle between the plane of the [Cp*] ligand and the plane of the bidentate PN ligand (the plane defined by the Rh, N and P atoms) is 60.5º, similar to the analogous angle (62.0º) in the structure of **2** supported by PQN.[15] This similarity suggests that the increased flexibility of the PN ligand does not markedly influence the geometry of the Rh center in **1**. In addition, the P–Rh–N bond angle does not differ significantly (<1º difference) between **1** and **2**, despite the greater rigidity enforced by the quinoline moiety within the PQN ligand of **2**. These similar structural features are consistent with the comparable Rh^{III}/Rh^{I} reduction potentials measured for **1** and **2** (*vide infra*).

However, comparison of the bond lengths of **1** and **2** reveal that the Rh–P bond in **1** is marginally shorter than that in **2**; the shorter bond length in **1** may again indicate that PN (at the P atom) is a stronger donor ligand and therefore engenders a more basic Rh center than that found in **2**. The more negative reduction potential of **1** versus **2** (*vide infra*) is also consistent with these structural findings.

3.3 Electrochemical studies

Past studies of [Cp*Rh] complexes supported by 2,2′-bipyridyl (bpy) derivatives[4,11,12] and dppb[10] have shown that electrochemical reduction of the compounds proceeds through a net $2e^-$ reduction from Rh^{III} to Rh^{I} via an ECE′-type mechanism (E = electron transfer, C = chemical reaction).[29] In such studies, initial reduction (E) leads to ejection of the monodentate ligand (usually chloride or solvent) (C) and thus a positive shift in $E(Rh^{II}/Rh^{I})$ such that it is positive of the $E(Rh^{III}/Rh^{II})$ associated with the starting compound. In our prior work, **2** was found display a similar electrochemical profile, undergoing reduction from Rh^{III} to Rh^{I} at –1.19 V vs $Fc^{+/0}$ (Figure 4, lower panel).[15] Unique to the PQN system, this $2e^-$ reduction is followed by a third reduction at –2.26 V vs. $Fc^{+/0}$, a feature that we have previously predicted to be PQN-ligand-centered on the basis of chemical reactivity.

We find that **1** displays similar electrochemical properties in comparison with these previously investigated systems. The cyclic voltammogram (CV) of **1** (Figure 4, upper panel) shows a single reduction event at –1.28 V vs $Fc^{+/0}$, consistent with a net $2e^-$ reduction from Rh^{III} to Rh^{I} *(vide infra)*. Evidently, the ECE′-type mechanism dominates the electrochemical behavior of **1** as it does with **2**,

consistent with the similar chelating nature and structural features of PN and PQN, respectively.

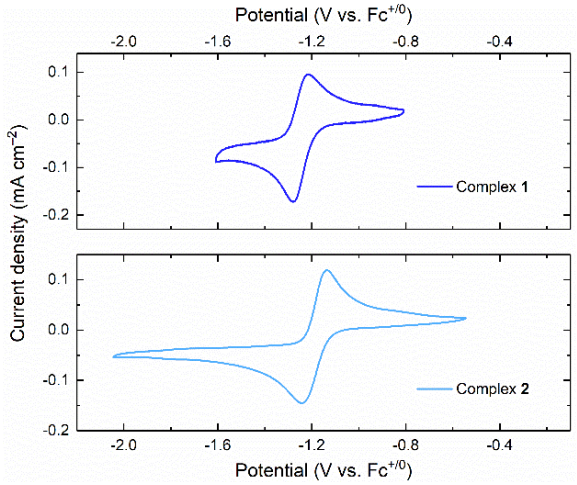

Figure 4. Cyclic voltammetry of **1** and **2**. Electrolyte: 0.1 M $TBAPF_6$ in acetonitrile; Scan rate: 100 mV/s; Working electrode: highly oriented pyrolytic graphite (HOPG); [Rh] in each experiment was ca. 1 mM. Initial potentials were ca. –0.8 V for **1** and ca. –0.6 V for **2**.

The CV profile of **1** is consistent with a sequence in which the chloride-bound Rh^{III} species undergoes $1e^-$ reduction to a transient 19-electron species. The expected subsequent loss of the Cl^- ligand (as occurs with **2**) would form a 17-electron complex that could undergo immediate transfer of a second electron, giving rise to a Rh^I product (**3**). We have assigned this sequence leading to generation of **3** on the basis of observed chemical reactivity (*vide infra*), along with the close similarity of the appearance of the electrochemical data for **1** with the prior systems we have studied in the [Cp*Rh] family. We also note that scan rate-dependent studies show that both **1** and **3** are freely diffusing in solution, consistent with their solubility in acetonitrile (see Supporting Information, Figure S14).

As mentioned above, **2** undergoes a third, one-electron reduction at –2.26 V that we have tentatively assigned as a reduction associated with PQN ligand.[15] Consistent with this theory, no third reduction is observed in the CV data for **1** (Figure 5). The extended conjugation of PQN due to the presence of the quinoline moiety is expected to give rise to this notable difference in accessible oxidation states, as expected on the basis of the reduction potentials for quinoline and pyridine.[30]

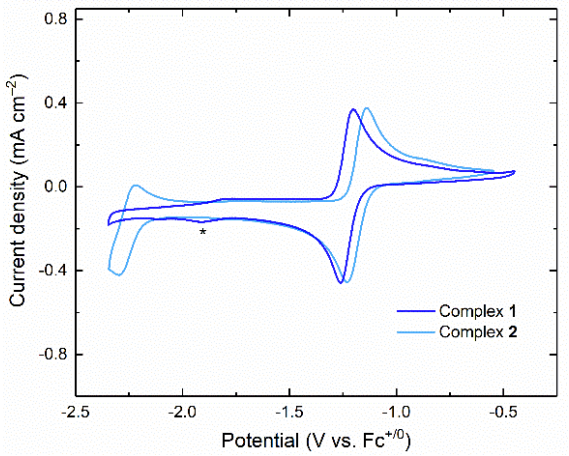

Figure 5. Comparison of CV data for **1** and **2**. Electrolyte: 0.1 M $TBAPF_6$ in acetonitrile; Scan rate: 100 mV/s; Working electrode: highly oriented pyrolytic graphite (HOPG); [Rh] in each experiment was ca. 1 mM. Initial potential: **1** and **2** ca. –0.5 V. * indicates reduction of a small impurity of $[Cp^*RhCl_2]_2$.[31]

Comparison of all the reduction potentials of the [Cp*Rh] complexes studied in our group to date reveals that **1** has the most negative Rh^{III}/Rh^I reduction potential yet accessed in our series.[10, 11,12,15] Comparing the most closely related cases of **1** and **2**, this finding agrees with the available structural data implicating a greater donor strength for PN in comparison with PQN. More broadly, **3** can be anticipated from the electrochemical work to be rather basic in nature due to the rather negative potential at which this compound is generated. Indeed, we find that **3** is quite basic on the basis of chemical reactivity observed upon chemical reduction (*vide infra*).

*3.4 Identification of the Product Mixture Resulting from Chemical Reduction of **1** Followed by Chemical Reactivity*

The electrochemical data suggest that a Rh^I complex, **3**, is formed upon two-electron reduction of **1** and is stable at least on the timescale of seconds-to-minutes, as interrogated by CV. To further investigate the nature of **3** and/or further chemical reactivity of this species, we targeted chemical reduction of **1** by treatment with sodium amalgam (Na(Hg)). This reductant was selected for its rather negative reduction potential ($E^o \approx -2.36$), sufficiently negative for reduction of **1** on the basis of the CV results.[32] Addition of a solution containing **1** in tetrahydrofuran to a vial containing

Na(Hg) results in a marked color change from orange to purple and eventually blue over the timescale of thirty minutes to an hour. From this rapid color change, we theorize that electron transfer from Na(Hg) to the starting compound **1** is relatively fast, a theory also supported by the electrochemically quasi-reversible voltammetry. Removal of THF solvent yields a dark blue solid that can be extracted and redissolved for characterization of products with ^{1}H NMR and ^{31}P{^{1}H} NMR.

Three rhodium species are detectable in the reaction mixture resulting from reduction of **1** with Na(Hg). ^{1}H NMR spectra shows two major sets of aromatic resonances in a 2:1 ratio (Figure S8). ^{1}H NMR also reveals accompanying aliphatic resonances corresponding to Cp* protons (relative to the aromatic protons, integrating to 30H and 15H, respectively) at 1.63 ppm ($J \approx 2.7$, 1.0 Hz) and 1.94 ppm ($J \approx 2.0$ Hz). These signals correspond to formation of two diamagnetic species bearing intact [η^5-Cp*] ligands, one of which is **3** (see Scheme 3). The ^{1}H NMR spectrum also features a unique doublet at 3.02 ppm ($^{2}J_{H,P}$ = 10.4 Hz); on the basis of proper integration, this doublet is associated with the species giving the [η^5-Cp*] resonance at 1.94 ppm (the relative integration of the specific *ortho*-pyridyl proton, Cp* protons, and methylene protons in this species is 1:15:2 protons). The integration of this doublet as 2H is consistent with formation of **3**, as the methylene protons on the bridge of the PN ligand of **3** are spectroscopically equivalent; this compares well with the known C_{2v} symmetry of related formally Rh^{I} compounds bearing bidentate chelating ligands.[15,33] This assignment is further supported by findings from the two-dimensional ^{1}H–^{1}H NMR techniques NOESY and COSY that confirm the expected coupling network for **3** (see Figures S11 and S12). Furthermore, ^{31}P{^{1}H} NMR features a large doublet at 61.1 ppm associated with **3**; the significant increase in coupling constant for this set of resonances ($^{1}J_{P,Rh} \approx 244.7$ Hz) in comparison with those associated with **1** ($^{1}J_{P,Rh} \approx$ 140.7 Hz) is consistent with reduction of the metal center upon formation of **3** from **1**.

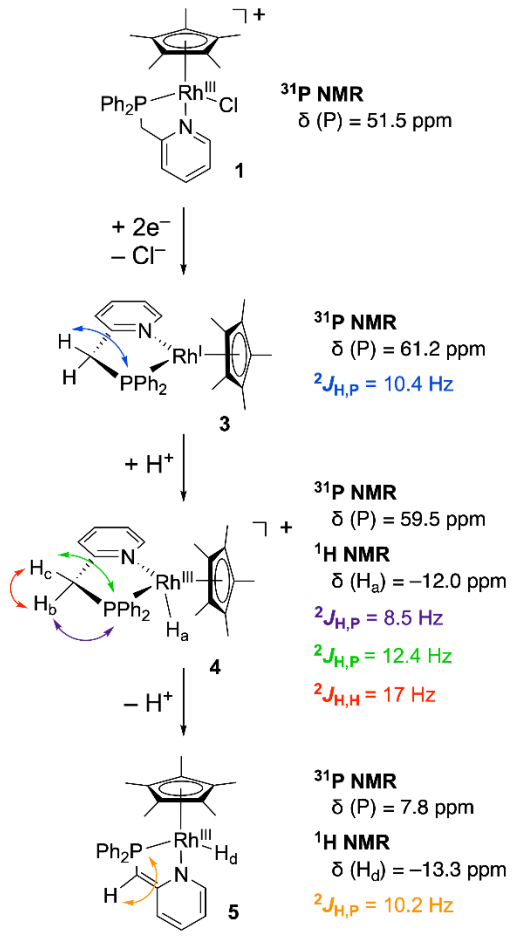

Scheme 3. Schematic reactivity of **1** upon reduction by Na(Hg).

The upfield region of the ^{1}H NMR collected on the mixture resulting from reduction of **1** with Na(Hg) features a doublet of doublets at –12.0 ppm that integrates as 1H with respect to the second full set of peaks associated with the [η^5-Cp*] signal at 1.63 ppm. This set of resonances indicates formation of the [Cp*Rh] hydride complex **4**; in particular, the distinctive doublet of doublets can be confidently ascribed to the hydride H-atom itself, as it displays the expected $^{1}J_{H,Rh}$ and $^{2}J_{H,P}$ couplings (40.8, 30.1 Hz). Also associated with **4**, two doublets of doublets of doublets appear in the aliphatic region of the ^{1}H NMR spectrum at 4.18 ppm ($J \approx$ 17.6, 12.4, 2.3 Hz) and 3.48 ppm ($J \approx$ 17.3, 8.5, 1.0 Hz), integrating in a 2:1 ratio with the hydride peak at –12.0 ppm. These resonances are associated with the expected methylene protons of the PN ligand bound to **4**; due to the *pseudo*-octahedral geometry of **4**, the protons on the bridging methylene unit in PN are diastereotopic.

This situation is similar to that encountered for the methylene protons in **1** (see Figure 1). Notably, the assignment of the formulation of **4** as a hydride bearing an unmodified PN ligand was confirmed by the two-dimensional NMR studies (Figure S11 and S12). Consistent with this model, the $^{31}P\{^{1}H\}$ NMR spectrum shows a second major doublet centered at 59.5 ppm corresponding to **4** with $^{1}J_{P,Rh} \approx 148.5$ Hz.

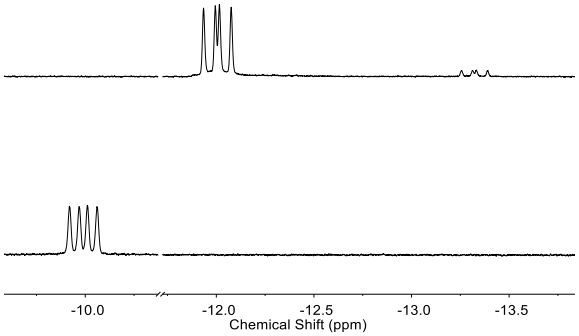

Figure 6. Upfield region of selected ^{1}H NMR spectra. Upper panel: chemical reduction of **1**; lower panel: $[Cp^*Rh(PQN)H]^{+}OTf^{-}$.

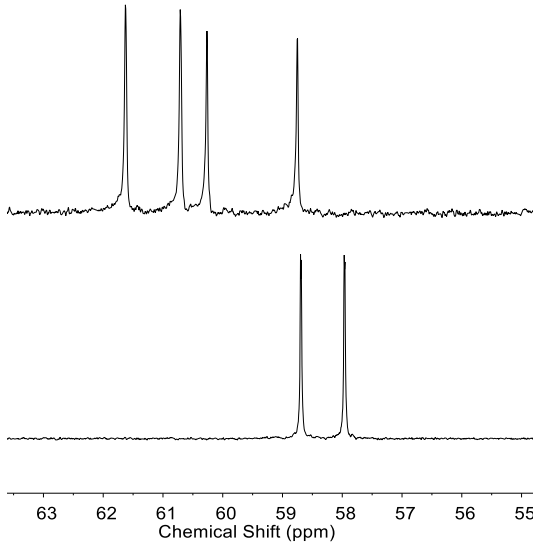

Figure 7. Partial $^{31}P\{^{1}H\}$ NMR spectra for the products of chemical reduction of **1** (upper) and $[Cp^*Rh(PQN)H]^{+}$ OTf (lower).

In addition to the large signals associated with the major products of reduction being **3** and **4**, an additional doublet of doublets is observed by ^{1}H NMR at –13.3 ppm (J = 38.5, 28.4 Hz). This signal indicates generation of a second, minor $[Rh^{III}–H]$ species, **5**. Indeed, re-inspection of the full ^{1}H NMR spectrum reveals an accompanying set of minor peaks in the aromatic region and a small $[\eta^5\text{-}Cp^*]$ peak at 1.39 ppm also associated with **5**. Most unique, a doublet appears at 3.84 ppm with $^{2}J_{H,P}$ = 10.2 Hz which integrates as 1H with respect to the hydride signal at –13.3 ppm; this doublet indicates that **5** bears an LX-type ligand derived from PN that is presumably generated by deprotonation of **4** by **3**. The $^{31}P\{^{1}H\}$ NMR spectrum of the mixture also displays an expected minor doublet associated with the hydride complex **5** at 7.81 ppm ($^{1}J_{P,Rh} \approx 195.4$ Hz; see Figure S10). As in the other cases, two-dimensional NMR studies confirm the full assignment of the structure of **5** (Figure S11 and S12). Notably, Norton and co-workers have examined similar [Cp*Rh] hydride complexes to **5** bearing LX-chelate ligands like 2-phenylpyridine.[34]

The hydride resonances associated with **4** and **5** are reminiscent of those we have measured for the $[Cp^*Rh(PQN)H]^{+}$ species generated by two-electron reduction of **2** followed by addition of anilinium triflate (pK_a = 10.6 in CH_3CN) as an exogenous proton source.[35] The ^{1}H NMR of this species displays an upfield set of resonances at –9.9 ppm appearing as a doublet of doublets due to H,Rh and H,P coupling ($J \approx 36.6$, 19.9 Hz). This is notably similar to the resonances observed for the hydride ligands of **4** (δ = –12.0 ppm, $J \approx 40.8$, 30.1 Hz) and **5** (δ = –13.3 ppm, J = 38.5, 28.4 Hz).

The electrochemical data showing reduction of **1** and generation of **3** do not indicate that chemical reactivity to form **4** and **5** occurs on the timescale of cyclic voltammetry. Therefore, this reaction must be rather slow, taking place over the timescale of tens of minutes to an hour and therefore not observable on the electrochemical timescale. However, based on the appearance of the CV data as well as the rapid color change from orange to purple and then eventually blue observed upon treatment of **1** with Na(Hg), electron transfer can be assumed to be reasonably fast.

Based on the observed products, **3** is capable of deprotonation of other species in solution. The most likely species to undergo deprotonation are rhodium-containing species, as deprotonation of the tetrahydrofuran solvent is unlikely due to its high intrinsic pK_a value. The two most likely endogenous proton sources are either the Rh^{III} starting material,

1, or a formally Rh^{II} species generated by reduction of **1**. Although the reduction of complex **1** is fast upon addition of Na(Hg), **1** has very poor solubility in tetrahydrofuran and becomes soluble only upon chemical reduction. This poor solubility could contribute to the simultaneous presence of both **3** and unreacted **1**, and enable **1** to serve as a proton source for generation of **4** from **3** in solution. The acidic protons of the backbone C–H bonds of the PN ligands would be present in both **1** and its one-electron reduced species; either of these could lead to generation of the major hydride product **4**. Similarly, the minor hydride **5** could be generated by deprotonation of nascent **4** by **3**.

Notably, the NMR spectra suggest that a greater quantity of **4** than **5** is produced. This is reasonable, in that the initial solution contains mostly **1** at the start of exposure to Na(Hg), favoring possible deprotonation of **1** by nascent **3**. Additionally, there could be a difference in acidity of the backbone C–H bonds of the PN ligands in **1** and **4**. As the hydride ligand in **4** is a more effective donor than the chloride ligand in **1**, the effective pK_a of the C–H bonds of PN could be correspondingly higher for **4** than for **1**, making **1** more acidic and giving a higher driving force for proton donation. Notably, however, we do not observe the immediate products of deprotonation of the starting material **1** or the analogous Rh^{II} species. Thus, other Rh species bearing a deprotonated form of the PN ligand may be tentatively concluded to undergo further reactivity and/or decomposition under the conditions of reduction by Na(Hg).

4. Conclusions

We have described the synthesis, characterization, electrochemical properties, and chemical reactivity profile of a [Cp*Rh] complex (**1**) bearing a hybrid, methylene-bridged κ^2-[*P*,*N*]-2-[(diphenylphosphino)methyl]pyridine ligand (PN). Electrochemical studies of **1** reveal a quasi-reversible two-electron reduction at –1.28 V vs $Fc^{+/0}$. This negative reduction potential corresponds to generation of the Rh^{I} complex **3**, a rather basic compound that, on the basis of chemical reactivity, can be concluded to be capable of deprotonation of the methylene C–H bonds of PN. Multiple products arise from this reactivity over a timescale of hours; these include two observable Rh^{III} hydride compounds with [η^5-Cp*] ligands but, noticeably, no compounds bearing [η^4-Cp*H] ligands. As the reduction of **1** results in the deprotonation of the acidic methylene C–H bonds and further speciation, this system is not amenable to further studies of H_2 generation during catalysis. Taken together, this work suggests that avoidance of acidic moieties in ancillary/supporting ligands[36] can be implicated as a winning strategy for improving the stability of complexes intended for study of H^+/e^- management during reductive catalysis.

5. Acknowledgements

The authors thank Dr. Justin Douglas and Sarah Neuenswander for assistance with NMR spectroscopy and Professor Kristin Bowman-James for helpful discussions. Synthesis and characterization of **1** was supported by the US National Science Foundation through the NSF REU Program in Chemistry at the University of Kansas (CHE-1560279). Reactivity studies were supported by the US National Science Foundation through award OIA-1833087. Support for NMR instrumentation was provided by NIH Shared Instrumentation Grants S10OD016360 and S10RR024664 and by the NSF MRI grant CHE-1625923.

This article is dedicated to Susan Teague, Bev Johnson, and Jan Akers in honor of their many years of distinguished service to the Department of Chemistry at the University of Kansas.

6. Notes

Corresponding Author

* To whom correspondence should be addressed. E-mail: blakemore@ku.edu, phone: +1 (785) 864-3019 (J.D.B.)

Present Address

† Department of Chemistry, Franklin & Marshall College, P.O. Box 3003, Lancaster, Pennsylvania, United States

7. References

[1] Lever, A. B. P., *Inorg. Chem.* **1990,** *29*, 1271-1285.

[2] (a) Rakowski Dubois, M.; Dubois, D. L., *Acc. Chem. Res.* **2009,** *42*, 1974-1982. (b) Appel, A. M.; Helm, M. L., *ACS Catalysis* **2013,** *4*, 630-633.

[3] (a) Khusnutdinova, J. R.; Milstein, D., *Angew. Chem. Int. Ed.* **2015,** *54*, 12236-12273. (b) Kaim, W.; Schwederski, B., *Coord. Chem. Rev.* **2010,** *254*, 1580-1588.

[4] (a) Kölle, U.; Grätzel, M., *Angew. Chem. Int. Ed. Engl.* **1987,** *26*, 567-570. (b) Kölle, U.; Kang, B. S.; Infelta, P.; Comte, P.; Grätzel, M., *Chem. Ber.* **1989,** *122*, 1869-1880.

[5] (a) Ruppert, R.; Herrmann, S.; Steckhan, E., *Tetrahedron Letters* **1987,** *28*, 6583-6586. (b) Ruppert, R.; Herrmann, S.; Steckhan, E., *J. Chem. Soc., Chem. Commun.* **1988**, 1150-1151. (c) Steckhan, E.; Herrmann, S.; Ruppert, R.; Dietz, E.; Frede, M.; Spika, E., *Organometallics* **1991,** *10*, 1568-77. (d) Lo, H. C.; Leiva, C.; Buriez, O.; Kerr, J. B.; Olmstead, M. M.; Fish, R. H., *Inorg. Chem.* **2001,** *40*, 6705-6716.

[6] Quintana, L. M. A.; Johnson, S. I.; Corona, S. L.; Villatoro, W.; Goddard, W. A.; Takase, M. K.; VanderVelde, D. G.; Winkler, J. R.; Gray, H. B.; Blakemore, J. D., *Proc. Nat. Acad. Sci. U.S.A.* **2016,** *113*, 6409-6414.

[7] Pitman, C. L.; Finster, O. N. L.; Miller, A. J. M., *Chem. Commun.* **2016,** *52*, 9105-9108.

[8] Johnson, S. I.; Gray, H. B.; Blakemore, J. D.; Goddard, W. A. *Inorg. Chem.* **2017**, *56*, 11375-11386.

[9] Todorova, T. K.; Huan, T. N.; Wang, X.; Agarwala, H.; Fontecave, M. *Inorg. Chem.* **2019**, *58*, 6893-6903.

[10] Boyd, E. A.; Lionetti, D.; Henke, W. C.; Day, V. W.; Blakemore, J. D., *Inorg. Chem.* **2019,** *58*, 3606-3615.

[11] Peng, Y.; Ramos-Garcés, M. V.; Lionetti, D.; Blakemore, J. D., *Inorg. Chem.* **2017,** *56*, 10824-10831.

[12] Henke, W. C.; Lionetti, D.; Moore, W. N. G.; Hopkins, J. A.; Day, V. W.; Blakemore, J. D., *ChemSusChem* **2017,** *10*, 4589-4598.

[13] (a) Klingert, B.; Werner, H. *Chem. Ber.* **1983**, *116*, 1450-1462. (b) Faller, J. W.; D'Alliessi, D. G. *Organometallics* **2002**, *21*, 1743-1746. (c) Faraone, F.; Bruno, G.; Schiavo, S. L.; Tresoldi, G.; Bombieri, G. *J. Chem. Soc., Dalton Trans.* **1983**, 433-438.

[14] (a) Jones, W. D.; Kuykendall, V. L.; Selmeczy, A. D. *Organometallics* **1991**, *10*, 1577-1586. (b) Edelbach, B. L.; Jones, W. D. *J. Am. Chem. Soc.* **1997**, *119*, 7734-7742.

[15] Hopkins, J. A.; Lionetti, D.; Day, V. W.; Blakemore, J. D., *Organometallics* **2019,** *38*, 1300-1310.

[16] (a) Carlson, B.; Eichinger, B. E.; Kaminsky, W.; Phelan, G. D. *The Journal of Physical Chemistry C* **2008**, *112*, 7858-7865. (b) Wei, S.; Pedroni, J.; Meißner, A.; Lumbroso, A.; Drexler, H.-J.; Heller, D.; Breit, B. *Chemistry – A European Journal* **2013**, *19*, 12067-12076. (c) de la Encarnación, E.; Pons, J.; Yáñez, R.; Ros, J. *Inorg. Chim. Acta* **2006**, *359*, 745-752. (d) Essoun, E.; Wang, R.; Aquino, M. A. S. *Inorg. Chim. Acta* **2017**, *454*, 97-106. (e) Murso, A.; Stalke, D. *Dalton Transactions* **2004**, 2563-2569. (f) Wei, D.; Bruneau-Voisine, A.; Chauvin, T.; Dorcet, V.; Roisnel, T.; Valyaev, D. A.; Lugan, N.; Sortais, J.-B. *Adv. Synth. Catal.* **2018**, *360*, 676-681. (g) Aakermark, B.; Krakenberger, B.; Hansson, S.; Vitagliano, A. *Organometallics* **1987**, *6*, 620-628. (h) Objartel, I.; Ott, H.; Stalke, D. *Z. Anorg. Allg. Chem.* **2008**, *634*, 2373-2379. (i) Aguirre, P. A.; Lagos, C. A.; Moya, S. A.; Zúñiga, C.; Vera-Oyarce, C.; Sola, E.; Peris, G.; Bayón, J. C. *Dalton Transactions* **2007**, 5419-5426. (j) Kermagoret, A.; Braunstein, P. *Organometallics* **2008**, *27*, 88-99. (k) Dubs, C.; Yamamoto, T.; Inagaki, A.; Akita, M. *Chem. Commun.* **2006**, 1962-1964. (l) Flapper, J.; Kooijman, H.; Lutz, M.; Spek, A. L.; van Leeuwen, P. W. N. M.; Elsevier, C. J.; Kamer, P. C. J. *Organometallics* **2009**, *28*, 1180-1192. (m) Sharp, P. R.; Hoard, D. W.; Barnes, C. L. *J. Am. Chem. Soc.* **1990**, *112*, 2024-2026. (n) Hung-Low, F.; Klausmeyer, K. K. *Inorg. Chim. Acta* **2008**, *361*, 1298-1310. (o) Mague, J. T.; Krinsky, J. L. *Inorg. Chem.* **2001**, *40*, 1962-1971. (p) A. Padron, D.; K. Klausmeyer, K. **2012**, *34*, 215–220. (q) Ma, A.-F.; Seo, H.-J.; Jin, S.-H.; Ung, C.; Yoon, M.; Ho, H.; Kwon Kang, S.; Kim, Y.-I. **2009**, *30*.

[17] (a) Wei, S.; Pedroni, J.; Meißner, A.; Lumbroso, A.; Drexler, H.-J.; Heller, D.; Breit, B. *Chemistry – A European Journal* **2013**, *19*, 12067-12076. (b) Wei, S.; Moller, S.; Heller, D.; Drexler, H.-J. *IUCrData* **2016**, *1*, x161318. (c) McNair, R. J.; Pignolet, L. H. *Inorg. Chem.* **1986**, *25*, 4717-4723.

[18] Groom, C. R.; Bruno, I. J.; Lightfoot, M. P.; Ward, S. C., *Acta Cryst. Sec. B* **2016,** *72*, 171-179.

[19] Brunner, H.; Kollnberger, A.; Mehmood, A.; Tsuno, T.; Zabel, M., *CSD Communication* **2009**, CCDC 233218, DOI: 10.5517/cc7tp5w

[20] (a) White, C.; Yates, A.; Maitlis, P. M., *Inorg. Synth.* **1992,** *29*, 228-234. (b) Mantell, M. A.; Kampf, J. W.; Sanford, M., *Organometallics* **2018,** *37*, 3240-3242.

[21] Hung-Low, F.; Klausmeyer, K. K. *Inorg. Chim. Acta* **2008**, *361*, 1298-1310.

[22] Fulmer, G. R.; Miller, A. J. M.; Sherden, N. H.; Gottlieb, H. E.; Nudelman, A.; Stoltz, B. M.; Bercaw, J. E.; Goldberg, K. I., NMR Chemical *Organometallics* **2010,** *29*, 2176-2179.

[23] (a) Harris, R. K.; Becker, E. D.; Cabral De Menezes, S. M.; Goodfellow, R.; Granger, P. *Pure Appl. Chem.* **2001,** *73*, 1795-1818. (b) Harris, R. K.; Becker, E. D.; Cabral De Menezes, S. M.; Granger, P.; Hoffman, R. E.; Zilm, K. W. *Pure Appl. Chem.* **2008,** *80*, 59-84.

[24] Data Collection: SMART Software in APEX2 v2014.11-0 Suite. Bruker-AXS, 5465 E. Cheryl Parkway, Madison, WI 53711-5373 USA.

[25] Data Reduction: SAINT Software in APEX2 v2014.11-0 Suite. Bruker-AXS, 5465 E. Cheryl Parkway, Madison, WI 53711-5373 USA.

[26] Refinement: SHELXTL Software in APEX2 v2014.11-0 Suite. Bruker-AXS, 5465 E. Cheryl Parkway, Madison, WI 53711-5373 USA.

[27] Aakermark, B.; Krakenberger, B.; Hansson, S.; Vitagliano, A. Organometallics **1987**, *6*, 620-628.

[28] Nutton, A.; Bailey, P. M.; Maitlis, P. M. J. Chem. Soc., Dalton Trans. 1981, 1997−2002.

[29] Saveant, J.-M., *Elements of Molecular and Biomolecular Electrochemistry*. Wiley: Hoboken, NJ, 2006.

[30] Tabner, B. J.; Yandle, J. R., *J. Chem. Soc. A: Inorg. Phys. & Theor.* **1968**, 381-388.

[31] Lionetti, D.; Day, V. W.; Lassalle-Kaiser, B.; Blakemore, J. D. *Chem. Commun.* **2018**, *54*, 1694-1697.

[32] Connelly, N. G.; Geiger, W. E., *Chem. Rev.* **1996,** *96*, 877-910.

[33] Blakemore, J. D.; Hernandez, E. S.; Sattler, W.; Hunter, B. M.; Henling, L. M.; Brunschwig, B. S.; Gray, H. B., *Polyhedron* **2014,** *84*, 14-18.

[34] (a) Hu, Y.; Li, L.; Shaw, A. P.; Norton, J. R.; Sattler, W.; Rong, Y. *Organometallics* **2012**, *31*, 5058-5064. (b) Hu, Y.; Norton, J. R. *J. Am. Chem. Soc.* **2014**, *136*, 5938-5948.

[35] Muckerman, J. T.; Skone, J. H.; Ning, M.; Wasada-Tsutsui, Y., *Biochim. Biophys. Acta Bioenerg.* **2013,** *1827*, 882-891.

[36] Lionetti, D.; Day, V. W.; Blakemore, J. D., *Dalton Trans.* **2019,** *48*, 12396-12406.